

The deterministic field-free magnetization switching of perpendicular ferrimagnetic Tb-Co alloy film induced by interfacial spin current

Cite as: Appl. Phys. Lett. **119**, 032409 (2021); <https://doi.org/10.1063/5.0052850>

Submitted: 01 April 2021 • Accepted: 14 July 2021 • Published Online: 21 July 2021

Yonghai Guo, Yunzhuo Wu, Yang Cao, et al.



View Online



Export Citation



CrossMark

ARTICLES YOU MAY BE INTERESTED IN

[Magnetization switching and deterministic nucleation in Co/Ni multilayered disks induced by spin-orbit torques](#)

Applied Physics Letters **119**, 032410 (2021); <https://doi.org/10.1063/5.0050641>

[Spin-orbit torques: Materials, physics, and devices](#)

Applied Physics Letters **118**, 120502 (2021); <https://doi.org/10.1063/5.0039147>

[Spin-orbit torque-induced magnetization switching in Pt/Co-Tb/Ta structures](#)

Applied Physics Letters **118**, 022401 (2021); <https://doi.org/10.1063/5.0035835>

 QBLOX



1 qubit

Shorten Setup Time

Auto-Calibration
More Qubits

Fully-integrated

Quantum Control Stacks
Ultrastable DC to 18.5 GHz
Synchronized <<1 ns
Ultralow noise



100s qubits

[visit our website >](#)

The deterministic field-free magnetization switching of perpendicular ferrimagnetic Tb-Co alloy film induced by interfacial spin current

Cite as: Appl. Phys. Lett. **119**, 032409 (2021); doi: [10.1063/5.0052850](https://doi.org/10.1063/5.0052850)

Submitted: 1 April 2021 · Accepted: 14 July 2021 ·

Published Online: 21 July 2021



View Online



Export Citation



CrossMark

Yonghai Guo, Yunzhuo Wu, Yang Cao, Xiaoxue Zeng, Bo Wang, Dezheng Yang,  Xiaolong Fan,  and Jiangwei Cao^{a)} 

AFFILIATIONS

Key Laboratory for Magnetism and Magnetic Materials of the Ministry of Education, Lanzhou University, Lanzhou 730000, People's Republic of China

^{a)} Author to whom correspondence should be addressed: caojw@lzu.edu.cn

ABSTRACT

Current-induced magnetization switching in compensated ferrimagnetic materials by the spin-orbit torque (SOT) effect is promising for the next generation information storage devices. In this work, we report the current-induced deterministic field-free magnetization switching of the perpendicular Tb-Co ferrimagnet layer in a Co/Ti/Tb-Co trilayers. We found that the switching proportion and polarity of the Tb-Co ferrimagnet depend on the magnetization direction of the in-plane Co layer. The switching process revealed by magneto-optical Kerr microscope imaging further confirmed the current-induced field-free switching of the Tb-Co layer. We also demonstrated the large SOT effective field and the perpendicular effective field acting on the Tb-Co layer, by utilizing the second harmonic voltage measurement and the current-induced loop shift method. The large interfacial SOT efficiency and deterministic field-free magnetization switching in the trilayers structure may accelerate the application of ferrimagnet in SOT memory devices.

Published under an exclusive license by AIP Publishing. <https://doi.org/10.1063/5.0052850>

Current-induced magnetization switching mediated by the spin torque effect in magnetic heterostructures has drawn much attention due to its potential application in information storage devices.¹⁻³ Although spin transfer torque (STT)-based magnetic random access memory (MRAM) has been commercialized recently, spin-orbit torque (SOT) offers several advantages over STT for the writing of information, since it allows for decoupling the write and read current channels, with great advantages in terms of endurance of the junction and switching speed relative to STT.^{4,5} For the storage unit of MRAM with perpendicular magnetic anisotropy (PMA), to achieve deterministic SOT-induced switching,^{6,7} an in-plane field along the current direction is normally required to break the symmetry of the system.⁸ It has been experimentally demonstrated that such a field can be generated within the devices by materials engineering, such as by utilizing the stray field from a ferromagnet (FM) layer in the device,⁹ or exchange coupling field from an adjacent antiferromagnet (AFM)¹⁰⁻¹³ or FM layer.^{14,15} Another approach for SOT-induced deterministic field-free switching PMA system is to utilize spin current with an out-of-plane component of spin polarization, which favors one perpendicular direction of the PMA layer and, therefore, can induce a

deterministic magnetization switching.^{16,17} Baek *et al.* experimentally proved that such a spin current can be produced at nonmagnetic (NM)/FM interface, and it is strong enough to induce a deterministic field-free magnetization switching in the adjacent PMA layer.¹⁸

From the viewpoint of materials, SOT-induced magnetization switching has been achieved in FM, AFM, and ferrimagnets systems. Although FM has been widely used as an information storage medium in traditional hard disk drives and state-of-the-art spintronic devices, AFM represents an exciting candidate for the next-generation information storage medium because it shows terahertz dynamics and the immunity to the stray field.¹⁹⁻²² These intrinsic properties of AFM offer advantages in writing speed and stability as an information storage medium. However, one main difficulty in the usage of AFM as an information storage medium is the lack of mechanisms for realizing efficient reading and writing. Recently, researchers have experimentally demonstrated the electrical control and probing of AFM by utilizing SOT and anisotropic magnetoresistance (AMR) effect,^{23,24} providing a solution for the difficulty mentioned above in antiferromagnet spintronics. Alternatively, the compensated ferrimagnets also exhibit ultrafast dynamics and strong immunity to the stray field, like

AFM.²⁵ Especially, in the rare earth (RE)-transition metal (TM) ferrimagnetic alloy,²⁶ a magnetic compensation point with a zero magnetization occurs for a certain alloy concentration or temperature.^{27,28} At this compensation point, RE-TM alloy exhibits similar magnetic behavior with AFM, while the magnetic-related transport properties in RE-TM are determined by the TM sublattice solely, which allow us to detect the magnetic states of a RE-TM alloy using similar electrical methods that have been traditionally used for FM, such as anomalous Hall effect (AHE)^{29,30} and magnetoresistance (MR) effect.

So far, the SOT effect in the NM/RE-TM structures has been studied by many groups;^{27,31–34} however, SOT-induced field-free magnetization switching has not been reported for RE-TM ferrimagnets. In this work, we report the deterministic field-free magnetization switching of perpendicular Tb-Co ferrimagnets induced by an in-plane current in Co (in-plane)/Ti/Tb-Co (PMA) trilayers. We find that the switching proportion and the polarity of the PMA Tb-Co ferrimagnet depend on the magnetization direction of the in-plane Co layer, suggesting the origin of the spin current from the Co layer or Co(-Tb)/Ti interface. Magneto-optical Kerr effect (MOKE) microscope imaging on the switching process revealed that the field-free switching of the Tb-Co layer is completed via the nucleation of reverse domain at the edge of Hall bar. The second harmonic voltage measurement demonstrated a large damping-like (DL) effective field acting on the Tb-Co ferrimagnetic layer due to the nearly compensated moment of Co and Tb atoms. In addition, the dependence of the out-of-plane effective field (H_z^{eff}) on the current amplitude demonstrated that the spin-orbit precession effect plays a key role for the field-free switching.

The film stacks shown in Fig. 1(a) were grown on thermally oxidized silicon wafer substrate by a magnetron sputtering system. A thin Ti layer (1 nm) was deposited as a seed layer for a good adhesion between film stacks and substrate. Then, a Co (3 nm)/Ti (3 nm)/Tb-Co (5 nm) trilayers structure was grown on the Ti adhesion layer. We choose this structure because the insertion of a Ti layer adds an additional Co/Ti interface, but as we know, the Ti layer itself has a

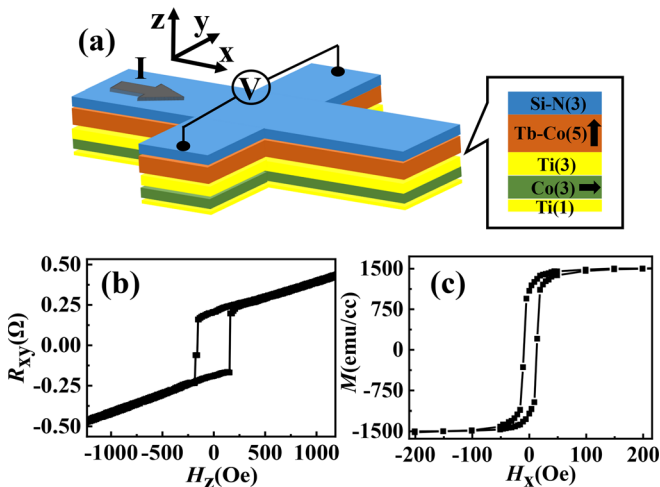


FIG. 1. (a) Schematic images of the Hall bar structure and film stack. (b) Hall resistance (R_{xy})- H_z and (c) M - H_x curve measured from the Co(3nm)/Ti(3nm)/Tb-Co(5 nm) structure.

negligible spin Hall effect.¹³ The Tb-Co alloy layer was grown by using the co-sputtering technique. The composition of the 5 nm-thick Tb-Co layer is optimized to be Tb_{0.28}Co_{0.72} (nominal composition), which exhibits low saturation magnetization ($M_s \approx 60$ emu/cc) and strong PMA at room temperature. Finally, a 3 nm-thick Si-N capping layer was deposited on the top for the protection of RE element from oxidation. After deposition, the film stack was patterned into Hall bar devices ($100 \times 10 \mu\text{m}^2$) by photolithography and ion milling techniques, as shown in Fig. 1(a).

The magnetic properties of the sample were characterized by vibrating sample magnetometer (VSM) and AHE. In the Hall resistance (R_{xy})- H_z curve, as shown in Fig. 1(b), the square hysteresis and the ramp part are contributed by the PMA ferrimagnetic Tb-Co layer and in-plane magnetized Co layer, respectively. The in-plane M_s - H_x loop of the full film stack was shown in Fig. 1(c). The in-plane magnetization is contributed mainly by the Co layer, in consideration of the strong PMA and the nearly compensated magnetization of the Tb-Co layer at room temperature (see supplementary material S1 for the temperature-dependent R_{xy} - H_z curves, from which the compensation temperature for the 5 nm-thick Co_{0.72}Tb_{0.28} layer was estimated to be around 240 K).

Next, we study the current-induced magnetization reversal of the PMA Tb-Co layer under various longitudinal fields (H_x). In this experiment, a series of current pulses with a pulse width of 1 ms were applied to the devices to switch their magnetization. Between two adjacent pulses, a small current of 1 mA was used to detect the magnetization states of the Tb-Co layer in the devices. The current-induced switching curves are shown in Figs. 2(a) and 2(b). Here, we use Hall

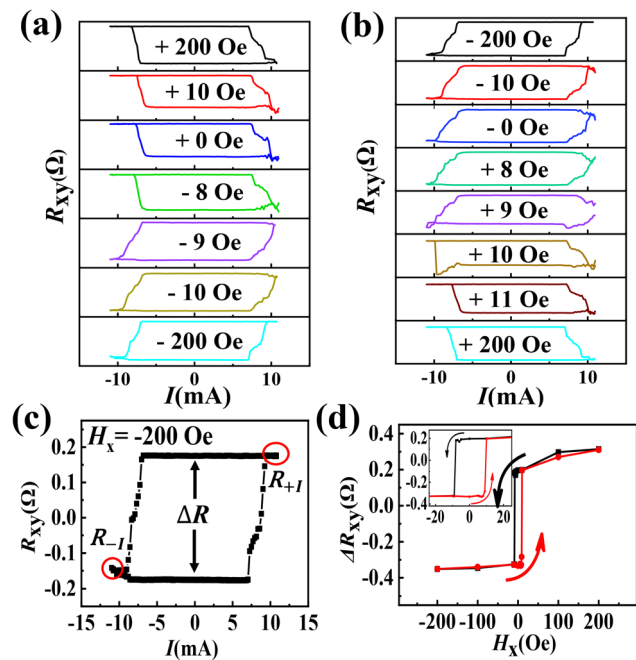


FIG. 2. Current-induced magnetization switching of the Tb-Co layer for various H_x with different sequence. H_x sweep from +200 to -200 Oe in (a) and with the reverse sequence in (b). (c) The definition of ΔR_{xy} in current-induced switching curve. (d) ΔR_{xy} vs H_x curve subtracted from (a) and (b).

resistance difference ΔR_{xy} ($\Delta R_{xy} = R_{-1} - R_{+1}$) to evaluate the switching proportion and polarity under different condition, where R_{-1} (R_{+1}) is the measured Hall resistance after the maximum negative (positive) current pulse, as schematically shown in Fig. 2(c). The positive (negative) ΔR_{xy} value represents the clockwise (counterclockwise) switching curve, and zero ΔR_{xy} hints no switching happening. We observe the deterministic magnetization switching of the PMA Tb-Co layer at the zero-field, and the switching polarity depends on the magnetization history of the in-plane Co layer. Quantitatively, the switching polarity changes at around -9 Oe ($+10$ Oe) when H_x varies from positive (negative) to negative (positive). The ΔR_{xy} vs H_x curve [Fig. 2(d)] exhibits a hysteresis-like behavior, and the “coercivity” (~ 9 Oe) is in accord with that of the M_x - H_x loop in Fig. 1(c). This quantitative identity of the “coercivity” values subtracted from ΔR_{xy} vs H_x and M_x - H_x loops further confirmed the fact that current-induced switching of PMA Tb-Co ferrimagnetic layer in the Co/Ti/Tb-Co trilayers depends on the magnetization state of the bottom in-plane Co layer, instead of the external field direction. This is totally different from the phenomenon observed in common heavy metal (HM)/FM and HM/FIM bilayer structures,^{5,35} where no switching happens at zero H_x , and the switching polarity reverses when H_x is reversed. In addition, we noted that ΔR_{xy} value in the zero-field switching is very close to that in field-induced switching, suggesting a complete and deterministic field-free switching in the Co/Ti/Tb-Co trilayers structure.

We also measured the current-induced magnetization switching with a transverse external field (H_y), or with an in-plane field with a fixed magnitude (100 Oe) but different azimuth angles (sweeping from $+x$ to $-x$ direction) (see supplementary material S2 for the detailed results), from which we discovered that the current-induced switching disappeared when the in-plane layer was saturated along the y direction. The results confirmed a fact that the current-induced switching of the Tb-Co layer relies on the magnetization state of the bottom Co layer.

To reveal the process for the field-free switching of PMA Tb-Co layer in this structure, we also performed microscopic magneto-optical Kerr effect (MOKE) imaging on a Hall-bar device during switching. In this experiment, the device was initially saturated by applying an out-of-plane pulse magnetic field (H_z), and then a series of short current pulses (15 mA in magnitude and 1–3 ms in duration for each pulse) were applied to the device. Between two current pulses, MOKE images were taken to monitor the magnetization state of the Tb-Co layer. In the entire switching and imaging processes, no in-plane field was applied. The corresponding MOKE images were shown in Fig. 3(a) for the switching from up to down, and the reverse process in Fig. 3(b). The MOKE microscope works in a differential model, and therefore, the gray area in the images represents upward (downward) magnetization, and the black (white) area represents downward (upward) magnetization if the sample is pre-saturated to upward (downward) magnetization. Note that the nucleation sites always appear at the top (bottom) edge of the stripe after a positive (negative) current, suggesting that the Oersted field plays a key role in the nucleation of the reversed domain.³⁶ In addition, the subsequent DW propagation is transverse (along y -direction), and finally, a complete magnetization reversal is achieved after hundreds of pulses. This is totally different from the HM/FM case, where no lateral domain wall propagation and deterministic switching happen at zero H_x field because of the Neel wall character induced by the Dzyaloshinskii-Moriya interaction

(DMI) at HM/FM interface.^{37,38} Taking into consideration of weak DMI at Ti/Tb-Co or Tb-Co/Si-N interface, the DW structure in the Tb-Co layer should exhibit Bloch type, and therefore, the spin current with y -direction polarization induces only transverse DW propagation. In addition, the observed deterministic field-free switching can also be explained by considering a current-induced out-of-plane effective field (H_z^{eff}) acting on the moments. We will discuss the origin of H_z^{eff} in detail subsequently.

To understand the current-induced spin torque effect in this trilayers structure, we used the second harmonic Hall voltage measurement method³⁹ to assess the SOT effective field acting on the Tb-Co layer. In this measurement, an a.c. current was applied to the Hall bar device; the variations of the second harmonics Hall resistance ($R_{2\omega}$) with H_x (H_y) were used to quantify the DL (field-like) field.⁴⁰ As shown in Fig. 4(b), $R_{2\omega}$ vs H_x shows a negative peak at a proper positive field, in consistent with the field dependence of the second harmonic measured for the Ta/FM sample previously, suggesting a negative effective spin Hall angle for the Co/Ti interface.¹⁸ Moreover, almost no signal is observed in the $R_{2\omega}$ vs H_y curve, indicating a negligible transverse effective field (the sum of the field-like and Oersted field) in this structure. Quantitatively, the damping-like (H_{DL}) and field-like effective field (H_{FL}) can be determined by the following expression:⁴¹

$$\Delta H_{x(y)} = \left(\frac{\partial R_{2\omega}}{\partial H_{x(y)}} \right) / \left(\frac{\partial^2 R_{\omega}}{\partial H_{x(y)}^2} \right), \quad (1)$$

$$H_{\text{DL}} = -2 \frac{(\Delta H_x \pm 2\xi \Delta H_y)}{1 - 4\xi^2}, \quad (2)$$

$$H_{\text{FL}} = -2 \frac{(\Delta H_y \pm 2\xi \Delta H_x)}{1 - 4\xi^2}, \quad (3)$$

$$\xi = \Delta R_{\text{p}} / \Delta R_{\text{A}}, \quad (4)$$

where ΔR_{p} and ΔR_{A} are the Hall resistances originating from the PHE and AHE, respectively. We measured the factor ξ in the Tb-Co layer from a separate Ti/Tb-Co/Si-N sample by scanning R_{H} vs in-plane applied field H with different field orientations,⁴² which is 0.033 ± 0.001 and, therefore, can be negligible in the calculation. Note that the “jump” near the zero-field in the $R_{2\omega}$ vs H_x curve originates from the anomalous Nernst signal,^{43,44} caused by the switching of the in-plane magnetized Co layer with H_x .¹⁸ To avoid the influence of the “jump” on the estimation of the SOT effective fields, we carried out linear fittings to the positive and negative low-field regions of the $R_{2\omega}$ vs H_x curve separately and averaged the results. We obtained the DL effective field $H_{\text{DL}} \approx -47.4$ Oe for $I = 4$ mA. The effective spin Hall angle $\theta_{\text{SH}}^{\text{eff}}$ is estimated by using the relation of $\theta_{\text{SH}}^{\text{eff}} = 2eM_{\text{S}}t_{\text{F}}H_{\text{DL}}/\hbar|j_e|$ which is -0.032 ± 0.002 , larger than that obtained from NiFe/Ti and CoFeB/Ti sample.¹⁸ The measured large H_{DL} suggests the existence of a spin current with the polarization along y -direction. Because the adjacent Ti layer is a light-metal with weak spin-orbit coupling, the large H_{DL} may originate from the spin Hall effect (SHE) of the Co layer,⁴⁵ or the Co/Ti interface by the spin-orbit filtering effect.¹⁷ Additional possible contribution from the Ti/Tb-Co interface cannot be excluded, as Cespedes-Berrocal *et al.* have found a large “self-torque” in GdFeCo/Cu sample, which can be enhanced by the adjacent spin sink layer.⁴⁶ However, as discussed previously, an external in-plane field is normally required to achieve deterministic SOT-induced

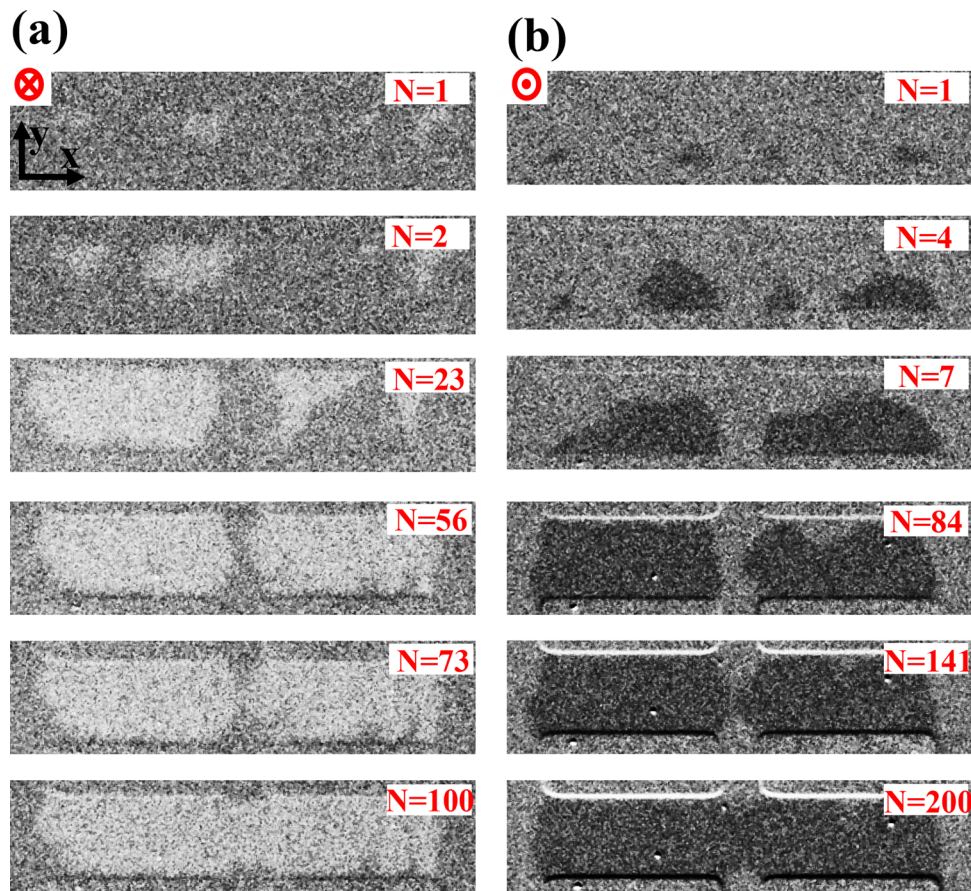


FIG. 3. MOKE images of a Hall bar device during current-induced magnetization reversal. The current pulses are 3 ms (1 ms) in duration for the left (right) column and 2.5×10^7 A cm $^{-2}$ in current density. Before applying the current pulses, the device was pre-saturated with a downward magnetization (left column) or upward magnetization (right column). The direction of H_z for pre-saturating the sample and the applied total pulse number before taking the images are given at the top left and top right of each panel, respectively. No external in-plane field is applied during the current pulses.

switching in the ordinary HM/FM (PMA) structures. Similarly, the measured large H_{DL} field caused by the spin current with y-polarization in the trilayers structure cannot induce the deterministic field-free switching of PMA layer solely and also cannot explain the dependence of the switching polarity on the magnetization direction of the bottom Co layer.

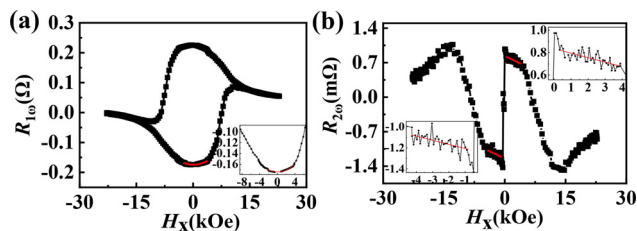


FIG. 4. (a) The first and (b) the second harmonic signals vs longitudinal swept field (H_x) from -23 kOe to $+23$ kOe. The red line shows the fitting to the measured curve.

Three different mechanisms have been proposed for the deterministic field-free switching in FM1 (in-plane)/NM/FM2 (PMA) trilayers structure: interlayer coupling,¹⁴ stray field,⁹ and spin-orbit precession effect.¹⁸ In the FM1 (in-plane)/NM/FM2 (PMA) trilayers structure, when the interlayer is thin enough, an effective in-plane coupling field acts on the PMA layer and break its symmetry, which may result in a deterministic switching in combination with the SOT effect.^{14,47} However, in considering of the “thick” interlayer ($t_{Ti} = 3$ nm) in this work, the coupling is quite weak and, therefore, cannot be considered as the main reason for the field-free switching. In addition, the stray field from the in-plane magnetized Co layer can also be excluded for the following two reasons. (1) The sample structure in our work cannot provide such a large stray field since we use a continuous FM layer, rather than a nano-pillar in Ref. 9. (2) Since the stray field supplies an AFM-like coupling field, the competition between the stray field and the external field will result in a multiple switching of the polarity in current-induced switching curve with various external field, which was not observed in our structure. To explain the observed current-induced field-free switching in this structure, we

need to consider the spin-orbit precession effect at Co/Ti interface. At the NM/FM interface, if the incoming current has a net polarization, the spin may change its orientation due to the spin-orbit precession effect.^{16–18} When the in-plane Co layer is magnetized along the x-direction, the spins are also polarized along the magnetization direction, which process around the spin-orbit coupling field (y-direction) at the NM/FM interface, resulting a net spin polarization along the z-direction. Such a spin current with z-polarization penetrates through the Ti layer and generates a DL torque on the perpendicular Tb-Co layer. In measuring the AHE curve with large current, this torque may compete with the applied perpendicular field (H_z) and induce a considerable shift along the H_z axis in the R_{xy} vs H_z loops. Fig. 5 shows the typical R_{xy} - H_z curves measured with different d.c. current (I_{dc}) and magnetization direction of the Co layer. We observe obvious loop shift with $I_{dc} = \pm 5$ mA [Figs. 5(a) and 5(b)], which relies on the current polarity and the magnetization direction of the bottom Co layer, while no loop shift appears with $I_{dc} = \pm 1$ mA [Fig. 5(c)]. The current amplitude dependence of the loop shift was summarized in Fig. 5(d). We clarify that the measured H_z^{eff} here is different from H_{DL} in Fig. 4; the former is relevant to the z-direction polarized spin current, while the latter is related to the y-direction polarized spin current resulting from bulk Co or interfacial spin-orbit effect. We noted that the current does not cause an obvious loop shift until it reaches a threshold above which the current-induced torque exceeds the intrinsic damping.¹⁸ This behavior is different from the linear dependence of the SOT-induced loop shift on the current density in the ordinary HM/FM system and cannot be caused by the interlayer coupling effect.⁴⁸ Therefore, we exclude the interlayer coupling effect and conclude that the spin current with z-polarization originating from spin-orbit precession effect at NM/FM interface is responsible for the current-induced field-free switching in the trilayers structures.

In summary, the current-induced deterministic field-free switching has been achieved in Co/Ti/Tb-Co trilayers structures. The switching polarity and proportion of the PMA Tb-Co ferrimagnet rely on

the x-component of the in-plane magnetized Co layer. A DL effective field measured from the second harmonic signal and the current-induced out-of-plane effective field suggest the existence of the y-polarization and z-polarization in the spin current. The former may originate from the Co layer or Co(-Tb)/Ti interface, while the latter can be explained by the spin-orbit precession effect at Co/Ti interfaces. The large SOT efficiency and field-free magnetization switching of FIM in the trilayers structure may accelerate the application of ferrimagnet in SOT memory devices.

See the [supplementary material](#) for the determination of the compensation temperature from the temperature dependence of the anomalous Hall effect (AHE) curves, and the current-induced magnetization switching in the Co/Ti/Tb-Co trilayers structure under different in-plane fields.

This work was supported by the National Natural Science Foundation of China (Nos. 11674142, 51771099, and 11774139) and by the Science and Technology Program of Gansu Province (No. 20JR5RA266).

DATA AVAILABILITY

The data that support the findings of this study are available from the corresponding author upon reasonable request.

REFERENCES

- ¹I. M. Miron, K. Garello, G. Gaudin, P. J. Zermatten, M. V. Costache, S. Auffret, S. Bandiera, B. Rodmacq, A. Schuhl, and P. Gambardella, *Nature* **476**, 189 (2011).
- ²L. Liu, C. F. Pai, Y. Li, H. W. Tseng, D. C. Ralph, and R. A. Buhrman, *Science* **336**, 555 (2012).
- ³C.-F. Pai, L. Liu, Y. Li, H. W. Tseng, D. C. Ralph, and R. A. Buhrman, *Appl. Phys. Lett.* **101**, 122404 (2012).
- ⁴K. Zhang, D. Zhang, C. Wang, L. Zeng, Y. Wang, and W. Zhao, *IEEE Access* **8**, 50792 (2020).
- ⁵S.-W. Lee and K.-J. Lee, *Proc. IEEE* **104**, 1831 (2016).
- ⁶L. Liu, O. J. Lee, T. J. Gudmundsen, D. C. Ralph, and R. A. Buhrman, *Phys. Rev. Lett.* **109**, 096602 (2012).
- ⁷L. Zhu, X. Xu, M. Wang, K. Meng, Y. Wu, J. Chen, J. Miao, and Y. Jiang, *Appl. Phys. Lett.* **117**, 112401 (2020).
- ⁸G. Yu, P. Upadhyaya, Y. Fan, J. G. Alzate, W. Jiang, K. L. Wong, S. Takeji, S. A. Bender, L. T. Chang, Y. Jiang, M. Lang, J. Tang, Y. Wang, Y. Tserkovnyak, P. K. Amiri, and K. L. Wang, *Nat. Nanotechnol.* **9**, 548 (2014).
- ⁹Z. Zhao, A. K. Smith, M. Jamali, and J. P. Wang, *Adv. Electron. Mater.* **6**, 1901368 (2020).
- ¹⁰M. Slezak, P. Drozd, W. Janus, H. Nayef, A. Koziol-Rachwal, M. Szpytma, M. Zajac, T. O. Mentes, F. Genuzio, A. Locatelli, and T. Slezak, *Nanoscale* **12**, 18091 (2020).
- ¹¹S. Fukami, C. Zhang, S. DuttaGupta, A. Kurenkov, and H. Ohno, *Nat. Mater.* **15**, 535 (2016).
- ¹²A. van den Brink, G. Vermijs, A. Solignac, J. Koo, J. T. Kohlhepp, H. J. M. Swagten, and B. Koopmans, *Nat. Commun.* **7**, 10854 (2016).
- ¹³Y.-W. Oh, S.-h Chris Baek, Y. M. Kim, H. Y. Lee, K.-D. Lee, C.-G. Yang, E.-S. Park, K.-S. Lee, K.-W. Kim, G. Go, J.-R. Jeong, B.-C. Min, H.-W. Lee, K.-J. Lee, and B.-G. Park, *Nat. Nanotechnol.* **11**, 878 (2016).
- ¹⁴Y. C. Lau, D. Betto, K. Rode, J. M. Coey, and P. Stamenov, *Nat. Nanotechnol.* **11**, 758 (2016).
- ¹⁵H. Wu, S. A. Razavi, Q. Shao, X. Li, K. L. Wong, Y. Liu, G. Yin, and K. L. Wang, *Phys. Rev. B* **99**, 184403 (2019).
- ¹⁶V. P. Amin and M. D. Stiles, *Phys. Rev. B* **94**, 104419 (2016).
- ¹⁷V. P. Amin, J. Zemen, and M. D. Stiles, *Phys. Rev. Lett.* **121**, 136805 (2018).

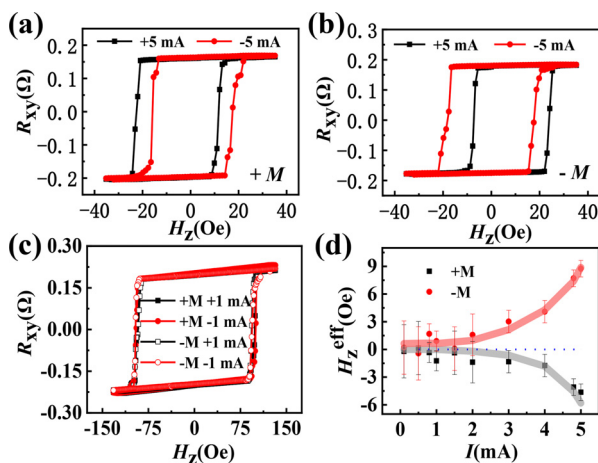


FIG. 5. Current-induced loop shift in the R_{xy} - H_z curves. (a) The R_{xy} - H_z curves measured with $I_{dc} = \pm 5$ mA with the device pre-magnetized along +x direction. (b) $I_{dc} = \pm 5$ mA with the device pre-magnetized along -x direction. (c) $I_{dc} = \pm 1$ mA with the device pre-magnetized along -x and +x directions. (d) The current amplitude dependence of the loop shift in the R_{xy} - H_z curves.

- ¹⁸S. C. Baek, V. P. Amin, Y. W. Oh, G. Go, S. J. Lee, G. H. Lee, K. J. Kim, M. D. Stiles, B. G. Park, and K. J. Lee, *Nat. Mater.* **17**, 509 (2018).
- ¹⁹T. Jungwirth, X. Marti, P. Wadley, and J. Wunderlich, *Nat. Nanotechnol.* **11**, 231 (2016).
- ²⁰G. Gurung, D.-F. Shao, and E. Y. Tsymlal, *Phys. Rev. B* **101**, 140405(R) (2020).
- ²¹T. Jungwirth, J. Sinova, A. Manchon, X. Marti, J. Wunderlich, and C. Felser, *Nat. Phys.* **14**, 200 (2018).
- ²²V. Baltz, A. Manchon, M. Tsoi, T. Moriyama, T. Ono, and Y. Tserkovnyak, *Rev. Mod. Phys.* **90**, 015005 (2018).
- ²³P. Wadley *et al.*, “Electrical switching of an antiferromagnet,” *Science* **351**, 587 (2016).
- ²⁴S. Y. Bodnar, L. Smejkal, I. Turek, T. Jungwirth, O. Gomonay, J. Sinova, A. A. Sapozhnik, H. J. Elmers, M. Klaui, and M. Jourdan, *Nat. Commun.* **9**, 348 (2018).
- ²⁵V. López-Flores, N. Bergéard, V. Halté, C. Stamm, N. Pontius, M. Hehn, E. Otero, E. Beaurepaire, and C. Boeglin, *Phys. Rev. B* **87**, 214412 (2013).
- ²⁶K. H. J. Buschow, *J. Appl. Phys.* **51**, 2795 (1980).
- ²⁷J. Finley and L. Liu, *Phys. Rev. Appl.* **6**, 054001 (2016).
- ²⁸P. Hansen, C. Clausen, G. Much, M. Rosenkranz, and K. Witter, *J. Appl. Phys.* **66**, 756 (1989).
- ²⁹N. Nagaosa, J. Sinova, S. Onoda, A. H. MacDonald, and N. P. Ong, *Rev. Mod. Phys.* **82**, 1539 (2010).
- ³⁰T. Jungwirth, Q. Niu, and A. H. MacDonald, *Phys. Rev. Lett.* **88**, 207208 (2002).
- ³¹T. H. Pham, S. G. Je, P. Vallobra, T. Fache, D. Lacour, G. Malinowski, M. C. Cyrille, G. Gaudin, O. Boule, M. Hehn, J. C. Rojas-Sánchez, and S. Mangin, *Phys. Rev. Appl.* **9**, 064032 (2018).
- ³²Z. Zhao, M. Jamali, A. K. Smith, and J.-P. Wang, *Appl. Phys. Lett.* **106**, 132404 (2015).
- ³³R. Q. Zhang, L. Y. Liao, X. Z. Chen, T. Xu, L. Cai, M. H. Guo, H. Bai, L. Sun, F. H. Xue, J. Su, X. Wang, C. H. Wan, H. Bai, Y. X. Song, R. Y. Chen, N. Chen, W. J. Jiang, X. F. Kou, J. W. Cai, H. Q. Wu, F. Pan, and C. Song, *Phys. Rev. B* **101**, 214418 (2020).
- ³⁴Y. Wu, X. Zeng, Y. Guo, Q. Jia, B. Wang, and J. Cao, *Appl. Phys. Lett.* **118**, 022401 (2021).
- ³⁵C. Zhang, S. Fukami, H. Sato, F. Matsukura, and H. Ohno, *Appl. Phys. Lett.* **107**, 012401 (2015).
- ³⁶J. C. Rojas-Sánchez, P. Laczkowski, J. Sampaio, S. Collin, K. Bouzehouane, N. Reyren, H. Jaffrès, A. Mougin, and J. M. George, *Appl. Phys. Lett.* **108**, 082406 (2016).
- ³⁷J. Cao, Y. Chen, T. Jin, W. Gan, Y. Wang, Y. Zheng, H. Lv, S. Cardoso, D. Wei, and W. S. Lew, *Sci. Rep.* **8**, 1355 (2018).
- ³⁸Y. Chen, Q. Zhang, J. Jia, Y. Zheng, Y. Wang, X. Fan, and J. Cao, *Appl. Phys. Lett.* **112**, 232402 (2018).
- ³⁹C. O. Avci, K. Garello, M. Gabureac, A. Ghosh, A. Fuhrer, S. F. Alvarado, and P. Gambardella, *Phys. Rev. B* **90**, 224427 (2014).
- ⁴⁰X. Qiu, Z. Shi, W. Fan, S. Zhou, and H. Yang, *Adv. Mater.* **30**, 1705699 (2018).
- ⁴¹M. Hayashi, J. Kim, M. Yamanouchi, and H. Ohno, *Phys. Rev. B* **89**, 144425 (2014).
- ⁴²S. Woo, M. Mann, A. J. Tan, L. Caretta, and G. S. D. Beach, *Appl. Phys. Lett.* **105**, 212404 (2014).
- ⁴³S. Y. Huang, W. G. Wang, S. F. Lee, J. Kwo, and C. L. Chien, *Phys. Rev. Lett.* **107**, 216604 (2011).
- ⁴⁴B. F. Miao, S. Y. Huang, D. Qu, and C. L. Chien, *AIP Adv.* **6**, 015018 (2016).
- ⁴⁵K. Kanagawa, Y. Teki, and E. Shikoh, *AIP Adv.* **8**, 055910 (2018).
- ⁴⁶D. Cespedes-Berocal, H. Damas, S. Petit-Watelot, D. Maccariello, P. Tang, A. Arriola-Cordova, P. Vallobra, Y. Xu, J. L. Bello, E. Martin, S. Migot, J. Ghanbaja, S. Zhang, M. Hehn, S. Mangin, C. Panagopoulos, V. Cros, A. Fert, and J. C. Rojas-Sanchez, *Adv. Mater.* **33**, 2007047 (2021).
- ⁴⁷W. Chen, L. Qian, and G. Xiao, *AIP Adv.* **8**, 055918 (2018).
- ⁴⁸Y. Sheng, K. W. Edmonds, X. Ma, H. Zheng, and K. Wang, *Adv. Electron. Mater.* **4**, 1800224 (2018).